DROPLET TRANSPORT IN HIGH REYNOLDS NUMBER WAKE FLOW

Ali Bagherpour
Department of Mechanical Engineering
University of New Brunswick
15 Dineen Drive, Fredericton, NB, Canada
Ali.Bagherpour@unb.ca

Gordon Holloway
Department of Mechanical Engineering
University of New Brunswick
15 Dineen Drive, Fredericton, NB, Canada
Holloway@unb.ca

ABSTRACT

This paper describes a study of droplet transport in high Reynolds number turbulent shear flow. A dilute polydisperse droplet spray was introduced into an axisymmetric disk wake with Re $\sim 6\times10^5$. The Reynolds number and droplet sizes used in this study cover a range of Stokes numbers $5 < St < 500$ and a mass loading of 10^{-2}. Data was gathered using a Phase Doppler Interferometer capable of measuring droplet size and 3 components of droplet velocity simultaneously. Results are sorted into 5 ranges of Stokes numbers and include wake profiles of droplet concentration, mean droplet velocity, and the dominant components of the droplet velocity fluctuation covariance.

INTRODUCTION

The turbulent transport of droplets is an essential element of many technological and environmental flows. Common examples include combustors and the dispersion of pesticides in the atmosphere. Engineering methods for the analysis of such flows are increasingly taking the form of RANS or LES based Computational Fluid Dynamics which requires models for the interaction of droplets with the continuous gas phase. However, a recent review of numerical and experimental methods for turbulent dispersed multiphase flow provided by Balachandar & Eaton (2010) draws attention to the need for measurements of size dependent droplet velocities and stresses to evaluate and develop such numerical models. Experiments for this purpose should have a simple form that emphasizes droplet interaction with sheared turbulence. Previous studies of this type include those of Ferrand *et al.* (2003) and Prevost *et al.* (1996) who considered an axisymmetric jet. Here we will describe results from an axisymmetric wake flow.

The wake flow has a Reynolds number, $\mathrm{Re} = U_{in}D/\nu_g \sim 6\times10^5$ where U_{in} is the unobstructed air velocity and D is the disk diameter. The distribution of droplets introduced into the wake have Stokes numbers, $5 < St < 500$ and sizes $0.1 < d/\eta_k < 4$ where $St = \tau_d/\tau_k$, $\tau_d = \rho_d d^2/18\mu_g$, τ_k is the Kolmogorov time scale and η_k is the Kolmogorov length scale. The Kolmogorov scales of the flow were estimated from the energy containing scales of the turbulence as: $\tau_k u'/l \sim \mathrm{Re}_l^{-0.5}$ and $\eta_k/l \sim \mathrm{Re}_l^{-0.75}$ where l is the integral length scale of the turbulence established as 10% of the wake half width and $\mathrm{Re}_l = u'l/\nu_g$. The values of St were calculated at each streamwise position based on the local turbulence level. The overall mass loading of the wake was $\alpha_m = \rho_l\Lambda_v \sim 0.01$ where Λ_v is the volume concentration of droplets. Measurements of 3 components of droplet mean velocity, 6 components of the Reynolds stress, plume aggregate and local droplet size spectra, the axial component of droplet flux and mean concentration profiles are reported at 2 streamwise locations, x/D =13.5 and 28.

EXPERIMENTAL APPARATUS

The wind tunnel used for the present study had a test section 1 m in diameter and 5 m in length. The air velocity was adjustable from 10 m/s to 85 m/s with the unobstructed tunnel airstream highly uniform and steady with a turbulence intensity, $u'/U_{in} < 1\%$.

The atomizer used to generate the droplets was attached to the front of the disk and both were supported by a streamlined strut which housed the fluid supply line. Fluid flow rate was measured by a precision turbine flow meter. The atomizer position relative to the measurement plane was adjustable between 0.15 m and 4.5 m. The atomizer used was a MicronAir AU6539 which is a rotary cage type. It had a 8.5 cm diameter and was electrically driven at 9500 rpm. The disk had a 14 cm diameter and a bevelled edge that faced downstream. In this configuration all droplets are introduced tangentially at the periphery of the disk with the large droplets traveling to larger radial distances owing to greater inertia. The blockage ratio $\pi D^2/4A_T = 2\%$, where A_T is the cross-sectional area of the tunnel test section.

All droplet size and velocity statistics were measured with an Artium Technologies PDI300. The PDI300 in the configuration used in this experiment was capable of measuring droplet size in the range $1\mu m < d < 600\mu m$ and 3-components of velocity in the range -100 to 160 m/s. It had two transmitter units that produce three beam pairs: green (532 nm), yellow (561 nm) and blue (473 nm). The measurement volumes of all 3 beam pairs had a maximum length of $\sim 600\mu m$. All measurements reported were calculated from fully coincident signals gathered from all 3 measurement volumes. The measurement volume was traversed across the spray with a high precision computer controlled

traverse mechanism.

Measurements of droplet size and velocity were made along horizontal and vertical lines at 2 measurement stations downstream of the atomizer. At each position the minimum velocity of the wake flow was detected and the droplet size and velocity were measured over the surrounding region having a sufficient droplet flux to provide adequate statistics. At each position either 100,000 droplets were measured or 100 seconds of data was gathered, whichever occurred first. A liquid flow rate of 1 l/min was used for all experiments.

Droplet Flux and Concentration

The PDI is a single particle counting instrument that records the size and velocity of each droplet which passes through its measurement volumes. The statistics of size and velocity are therefore gathered from a temporal sample and are correlated to particle-rate (Albrecht *et al.*, 2003). The arrival rate of droplets is approximately Poisson distributed as illustrated in Figure 1 for droplets with $St < 25$. In the event that 2 or more droplets are present in the measurement volume simultaneously a "rejection" is recorded. The data rate, $\lambda\,(\#/s)$, ranged from $\lambda = 10 - 10^4$ depending on the measurement position. Rejections, R, were less than 10% and corrections were applied on the assumption that the "accepted" data formed an unbiased sample.

Concentration, $\Lambda\left(\#/m^3\right)$, is based on a spatial sample and therefore must be inferred from temporal samples using the transformation $\Lambda = \lambda/UA$ where U is mean droplet velocity of a given size class and A is the cross-sectional area of the measurement volume which also depends on droplet size. Radial profiles of droplet flux, Φ, and droplet number concentration, Λ, are shown in Figures 2 and 3 respectively. The volume concentration profiles for different droplet St classes, $\Lambda_v\left(m^3/m^3\right)$, are shown in Figure 4. The maximum volume concentration for all Stokes number ranges occurs on the wake centerline and has a range of $10^{-8} < \Lambda_v < 10^{-5}$ which indicates that the droplets are dilute. This corresponds to a mass loading, $\alpha_m\left(kg/m^3\right)$, in the range, $10^{-5} < \alpha_m < 10^{-2}$. This implies that the interaction between the particles is negligible although the interaction between the particles and the flow turbulence may be significant (Elghobashi, 2006). Particles with $0 < St < 25$ had, by far, the greatest concentration although they displaced a relatively small volume compared to those in the range $200 < St < 400$.

The aggregate droplet size spectrum for the entire wake at both streamwise positions is shown in Figure 5. The two distributions are similar suggesting that the overall droplet population is stable. Figure 6 shows the radial profiles of surface mean diameter, d_{20}, at the two streamwise positions. At x/D =13.5, the smaller size droplets dominate the center of the near wake while larger droplets dominate the outer edges. This segregation originates from the tangential momentum of the droplets when released from the spinning sprayer. The segregation is diminished at $x/D = 28$ by turbulent transport.

Velocimetry

Radial profiles of mean axial droplet velocity, U, for 5 different ranges of St are shown on Figure 7. At both streamwise positions the mean droplet velocity has a deficit typical of wake flow as shown in Figure 8. The uncertainty of the velocity measurements is $\pm 0.1\%$. The scatter in the mean velocity plots mostly originates from asymmetries

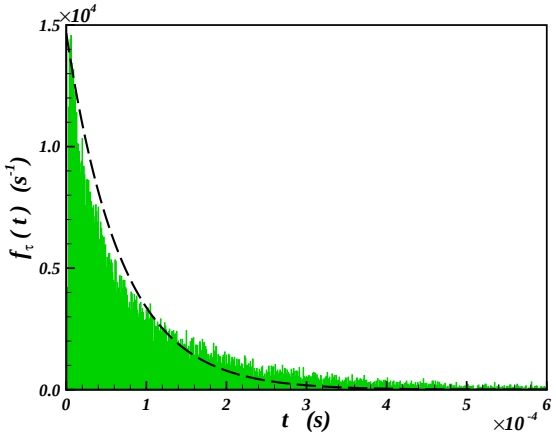

FIGURE 1. The probability density function of inter-arrival times, τ, for droplets in Stokes number class $St < 25$. The dashed line shows the exponential distribution with data rate corrected for rejections (10%).

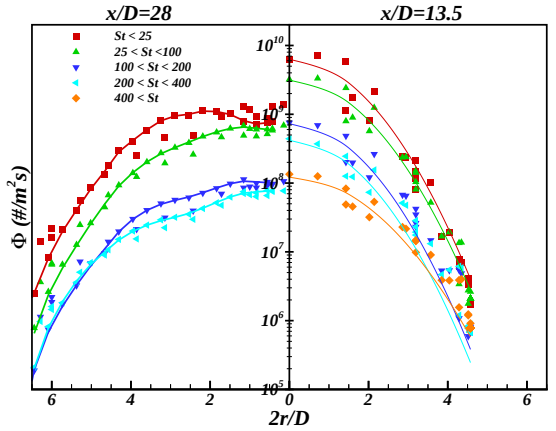

FIGURE 2. Radial profiles of droplet flux in the wake of the disk for 5 ranges of Stokes number. The right half of the figure corresponds to x/D =13.5 and the left to x/D =28.

of the flow. The radial mean droplet velocity, U_r, was less than 4% of the axial velocity. The mean tangential droplet velocity, U_θ, in this flow was practically zero.

Radial profiles of the RMS droplet velocity fluctuations: u', u'_r and u'_θ, are shown in Figures 9, 10 and 11. Values have been normalized by the centerline mean velocity deficit, U_0, of the wake at each streamwise position. In all cases, the RMS values are greater for the smaller St ranges. Near the centerline these velocity components are of similar magnitude but in the region of strong shear $u' > u'_r \sim u'_\theta$.

Radial profiles of the droplet velocity covariance, $\overline{uu_r}$, are shown in Figure 12. The maximum value of $\overline{uu_r}/U_0^2$ occurs for the smallest Stokes number range and decreases as Stokes number increases. For reference the radial gradient of mean axial velocity is also shown. The peak value of $\overline{uu_r}/U_0^2$ is displaced from the maximum shear rate by an amount that depends on St.

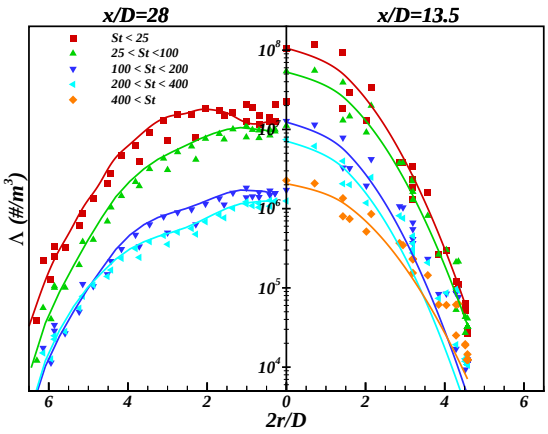

FIGURE 3. Radial profiles of droplet concentration in the wake of the disk for 5 ranges of Stokes number.

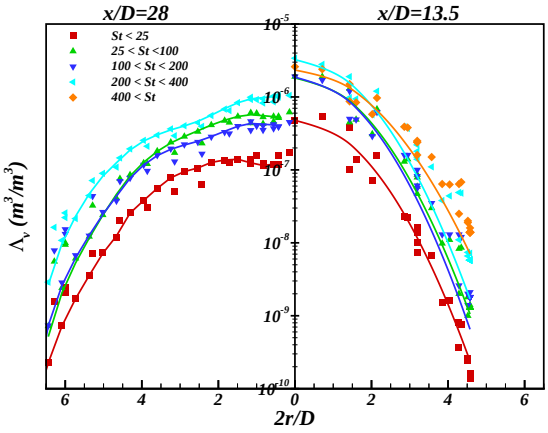

FIGURE 4. Radial profiles of droplet volume concentration in the wake of the disk for 5 ranges of Stokes number.

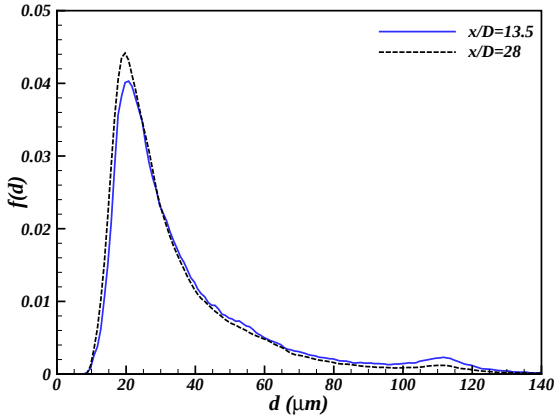

FIGURE 5. Aggregate droplet size distribution for the entire wake cross section at x/D =13.5 and 28. Droplets are produced by MicronAir AU6539.

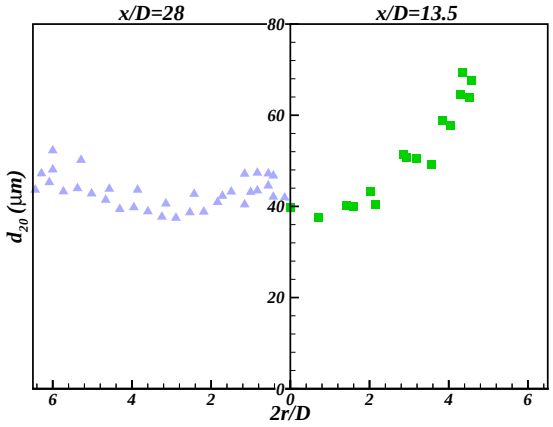

FIGURE 6. Profiles of surface mean diameter, d_{20}, in the wake of the disk at $x/D = 13.5$ and 28.

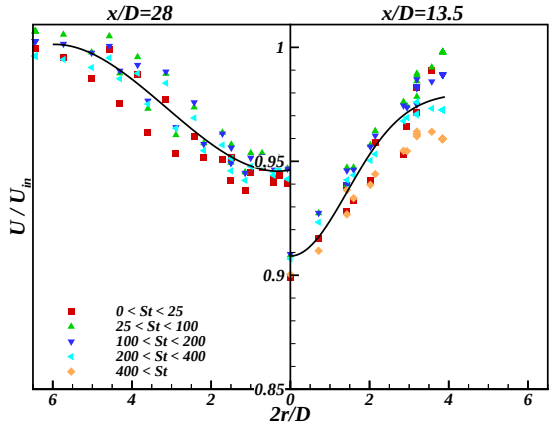

FIGURE 7. Radial profiles of mean streamwise droplet velocity, U, in the wake of the atomizer. Values are normalized by the unobstructed velocity at the test section inlet, $U_{in} = 65m/s$.

Profiles of $\overline{uu_r}/u'u'_r$ are shown in Figure 13. For $St < 25$ the peak value of correlation coefficient, $\overline{uu_r}/u'u'_r \approx$-0.40, whereas for $St > 400$ it has a value of -0.6. The larger values of $|\overline{uu_r}/u'u'_r|$ at higher Stokes number are in part due to the reduced energy of the droplets having the larger values of St as shown in Figures 9, 10 and 11.

DISCUSSION

It is generally suggested that when the droplet time scale, $\tau_d < 0.1l/u'$, droplets can follow the turbulent velocity of the flow with errors below 1% (Tropea *et al.*, 2007). In the present flow the droplets in the smallest range of Stokes number, $St < 25$, we have $\tau_d u'/l < 0.25$. Therefore, one would expect that droplets of this flow deviate to some extent from the energy containing scales of gas phase turbulence. To test this, we can compare velocity results for droplets having $St < 25$ to the single phase disk wake of Johansson & George (2006) with a Reynolds

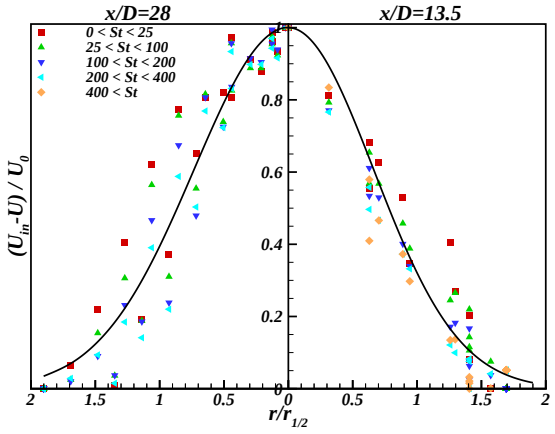

FIGURE 8. Radial profiles of normalized mean streamwise droplet velocity in the wake of the atomizer. The abscissa is normalized by the half width, $r_{1/2}$, of the mean velocity profile. The solid lines represent Gaussian curves fit to all size classes.

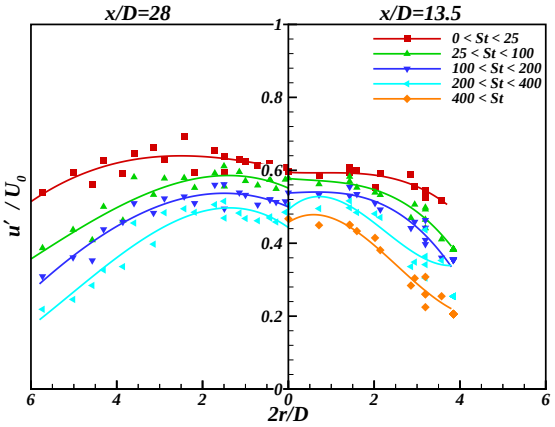

FIGURE 9. Radial profiles of RMS droplet velocity fluctuations in the axial direction in the wake of the atomizer. Values are normalized by the local centerline mean velocity deficit.

number of 36,000. The development of the centerline velocity deficit and half width of the wake are shown in Figure 14. The trends of the present data are comparable but at $x/D = 28$ the wake is significantly stronger and narrower than the single phase case. The shape of the mean velocity deficit is compared in Figure 15 where the radial distance has been normalized by the length scale

$$\delta^2 = \lim_{\tilde{r}\to\infty} \frac{1}{U_0} \int_0^{\tilde{r}} (U_\infty - U)\, r dr \qquad (1)$$

The deficit of momentum evaluated using the momentum thickness, $\theta^2 U_\infty^2$, differed by 5.5% between $x/D = 13.5$ and 28.

The droplet velocity fluctuation statistics of the Stokes number

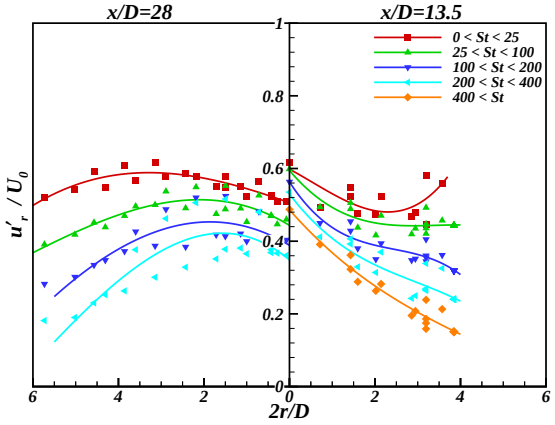

FIGURE 10. Radial profiles of RMS droplet velocity fluctuations in radial direction in the wake of the atomizer. Values are normalized by the local centerline mean velocity deficit.

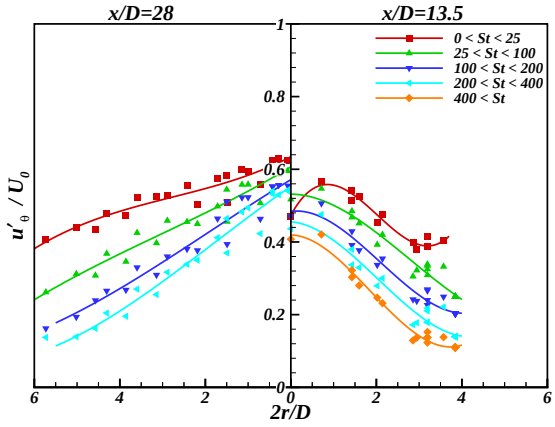

FIGURE 11. Radial profiles of RMS droplet velocity fluctuations in tangential direction in the wake of the atomizer. Values are normalized by the local centerline mean velocity deficit.

range $St < 25$ are compared to those of single phase flow statistics for wake flow in Figure 16. The profiles of RMS values in the axial direction normalized with the velocity deficit show significantly lower values than the single phase disk wake flow. However, the shear correlation coefficient has a value of $\overline{uu_r}/u'u'_r \sim -0.4$ which is typical of axisymmetric wake flow (Tennekes & Lumley, 1972).

It was shown in Figures 9 to 12 that the droplet velocity fluctuation statistics of the higher Stokes number ranges have progressively less energy. One interpretation being that at higher Stokes numbers the droplets are unable to follow the higher frequency turbulence motions. This has implications for the momentum transported by droplets. The turbulent transport coefficient, $\nu_d = \left|\overline{uu_r}/\left(\frac{\partial U}{\partial r}\right)\right|$, for droplets of different Stokes numbers was calculated at x/D =28 to be in the range $0.017 < \nu_d/U_0 r_{1/2} < 0.027$ with the lower values being for droplets with higher Stokes number. In a single phase axisymmetric wake $\nu_d/U_0 r_{1/2} \sim$

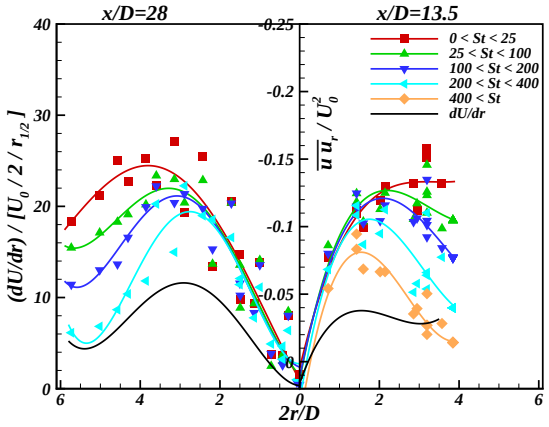

FIGURE 12. Radial profiles of droplet velocity fluctuation covariance in the wake of the atomizer. Profiles of the radial gradient of mean axial velocity for $St < 25$ are shown for reference.

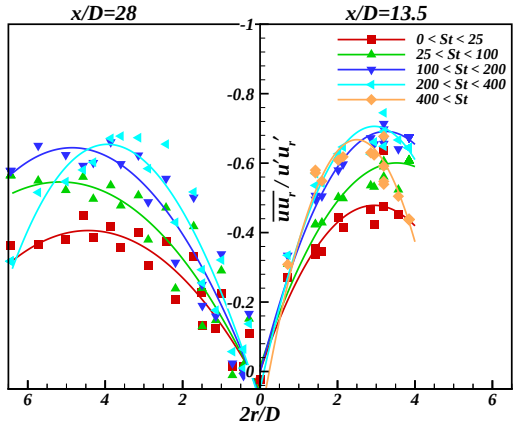

FIGURE 13. Radial profiles of the shear correlation coefficient, $\overline{uu_r}/u'u'_r$, in the wake of the atomizer.

0.05 (Hinze, 1975). The ratio of eddy viscosities, $\nu_d/(\nu_d)_{St<25}$, is shown in Figure 17 as a function of Stokes number. The ratio of momentum transported by the turbulent motion of the liquid phase to the gas phase in this flow is, $\beta = [\rho_l \Lambda_v (\overline{uu_r})_d] / \left[\rho_g (1-\Lambda_v)(\overline{uu_r})_g\right]$. This ratio for the largest St range was estimated to be $10^{-3} < \beta < 10^{-2}$ in this set of experiments.

The transport of the droplets down the concentration gradient is sometimes modeled according to gradient transport theory (Horender & Hardalupas, 2009) where a eddy diffusivity, D_t, is taken as proportional to the gas phase turbulence length and velocity scales. The normalized concentration profile for the present wake flow at x/D =28, all Stokes numbers combined, is shown in Figure 18. The velocity deficit is shown for comparison. The radial profile of concentration is approximately Gaussian in shape; however the half width of the concentration is less than the velocity deficit half width, $\left(r_{1/2}\right)_{vel}$. This implies that the

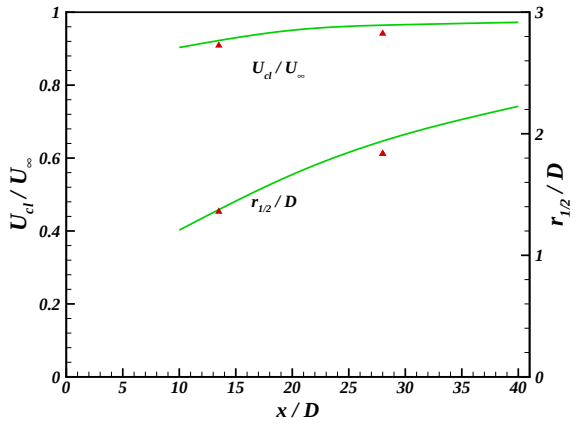

FIGURE 14. Downstream evolution of the centerline droplet mean velocity and wake half-width. Results based on droplets with $St < 25$. Solid lines show the data of Johansson & George (2006).

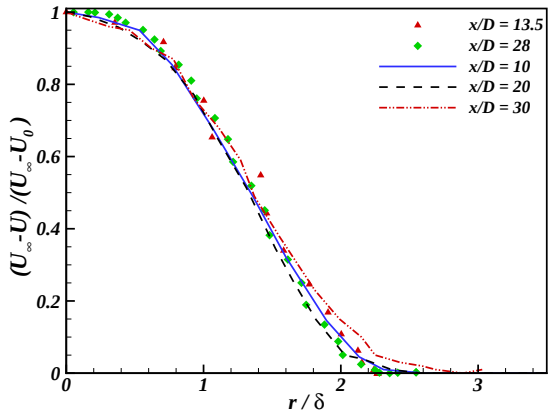

FIGURE 15. Radial profiles of droplet mean velocity deficit in the wake of the disk. Results based on droplets with $St < 25$. Lines indicate the data of Johansson & George (2006). Symbols represent average values at each radial position.

length scale of droplet transport differs from the momentum transport. A result that requires further study.

SUMMARY

The dilute droplet laden axisymmetric wake flow described in this study had a mean velocity deficit (for droplets having $St < 25$) that was similar to a single phase wake flow. However, the velocity and length scales of the present flow are evolving more slowly than in the single phase case.

The velocity statistics of the turbulent droplet motion depends on Stokes number but for all ranges it is less energetic, relative to the mean velocity deficit, than single phase wake turbulence. The droplets with the highest Stokes numbers have the lowest energy.

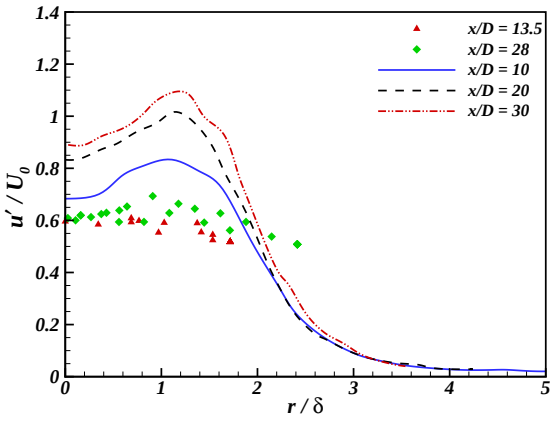

FIGURE 16. Radial profiles of axial velocity fluctuation in the wake of the disk. Results based on droplets with $St < 25$. Solid and dashed lines show the data of Johansson & George (2006). No correction for intermittency was applied to the data.

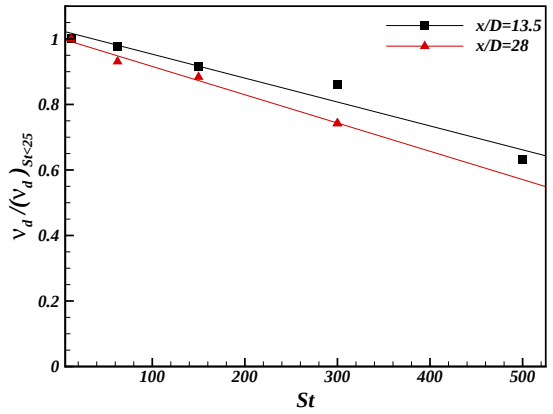

FIGURE 17. Average values of droplet transport from the shear layer as a function of Stokes number. Values are normalized by those of the smallest Stokes number range.

The statistical structure of the droplet motion, for $St < 25$, as measured by the ratio of normal stresses and the shear correlation coefficient, is very similar to a single phase wake. At higher Stokes numbers the shear correlation coefficient increases substantially in value. Both lower energy of motion and higher correlation coefficient for droplets with high Stokes number are consistent with the concept of droplet inertia "low-pass" filtering the gas phase motion of sheared turbulence. Overall, the turbulent momentum transport coefficient was found to decrease with increasing Stokes number.

The droplet concentration profiles were found to be approximately Gaussian in shape; however, the half width of the concentration profiles was approximately $\sim 80\%$ of the mean momentum half width at x/D =28. This is a significantly different outcome than for passive scale transport where the concentration half width is larger than that of the momentum deficit.

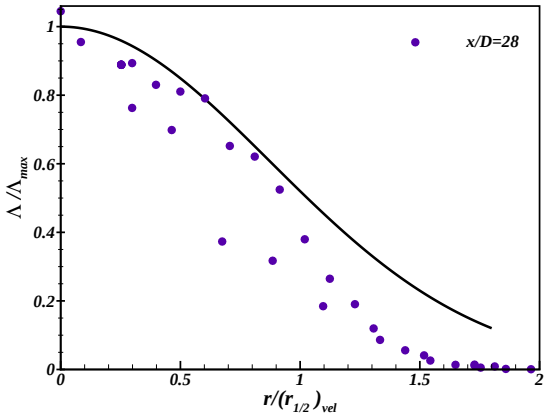

FIGURE 18. Radial profile of droplet concentration in the wake of the disk at x/D =28. Solid line shows the Gaussian fit to the velocity deficit of Figure 8.

Future work will include uniformly seeding the flow with smaller droplets and using larger droplet sizes to extend the range of Stokes numbers.

References

Albrecht, H. E., Borys, M., Damasche, N. & Tropea, C. 2003 *Laser doppler and phase doppler measurement techniques*. Springer.

Balachandar, S. & Eaton, J.K. 2010 Turbulent dispersed multiphase flow. *Annual Review of Fluid Mechanics* **42**, 111–133.

Elghobashi, S. 2006 An updated classification map of particle-laden turbulent flows. In *IUTAM Symposium on Computational Approaches to Multiphase Flow* (ed. R. Moreau, S. Balachandar & A. Prosperetti), *Fluid Mechanics and Its Applications*, vol. 81, pp. 3–10. Springer Netherlands.

Ferrand, V., Bazile, R., Boree, J. & Charnay, G. 2003 Gas-droplet turbulent velocity correlations and two-phase interaction in an axisymmetric jet laden with partly responsive droplets. *International Journal of Multiphase Flow* **29**, 195–217.

Hinze, J. O. 1975 *Turbulence*. New York: McGraw-Hill.

Horender, S. & Hardalupas, Y. 2009 Turbulent particle mass flux in a two-phase shear flow. *Powder Technology* **192**, 203 – 216.

Johansson, P. B. V. & George, W. K. 2006 The far downstream evolution of the high-reynolds-number axisymmetric wake behind a disk. part 1. single-point statistics. *Journal of Fluid Mechanics* **555**, 363–385.

Prevost, F., Boree, J., Nuglisch, H.J. & Charnay, G. 1996 Measurements of fluid/particle correlated motion in the far field of an axisymmetric jet. *International Journal of Multiphase Flow* **22** (4), 685–701.

Tennekes, M. & Lumley, J. L. 1972 *A First Course in Turbulence*. MIT Press.

Tropea, C., Foss, J. F. & Yarin, A. L. 2007 *Springer Handbook of Experimental Fluid Mechanics*. Berlin, Heidelberg: Springer.